

Supporting Information

Luminescent Metal-Organic Complexes of Pyrene or Anthracene Chromophores: Energy Transfer Assisted Amplified Exciplex Emission and Al³⁺ Sensing

Ritesh Haldar,^a Komal Prasad,^a Pralok Kumar Samanta,^b Swapan Kumar Pati^{ab} and Tapas Kumar Maji^{ac*}

Molecular Materials Laboratory, New Chemistry Unit,^a Chemistry and Physics of Materials Unit,^c Jawaharlal Nehru Centre for Advanced Scientific Research, Jakkur, Bangalore, 560064, India.

Theoretical Science Unit,^b Jawaharlal Nehru Center for Advanced Scientific research, Jakkur, Bangalore, 560064, India.

*E-mail address: tmaj@jncasr.ac.in, FAX: 91-80 22082766

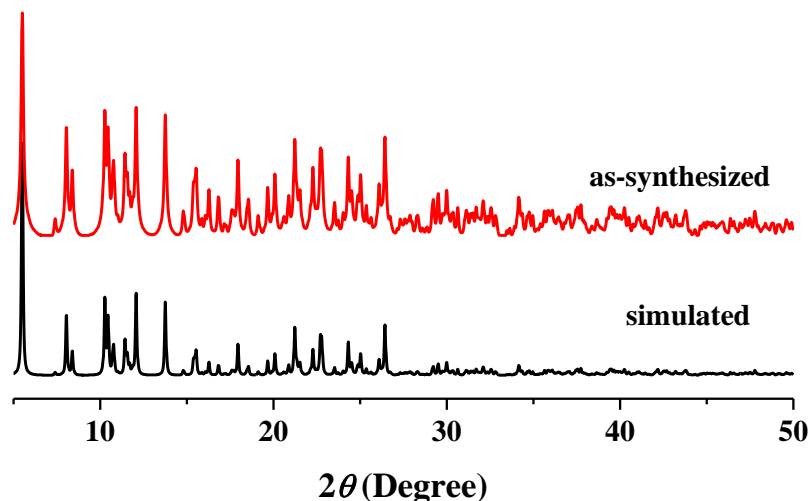


Figure S1. Simulated and as-synthesized PXRD patterns of compound **1**.

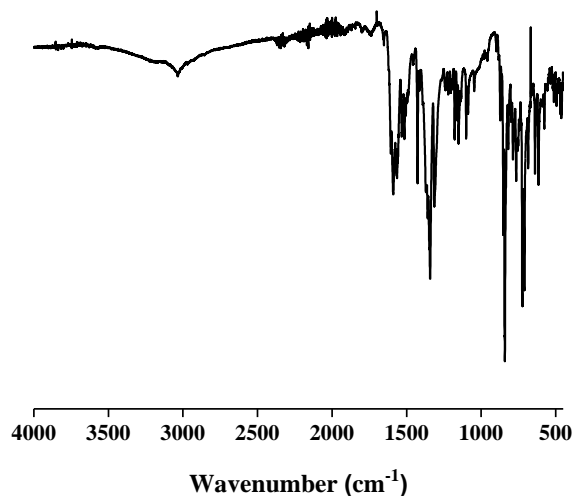


Figure S2. FT-IR spectrum of **1**.

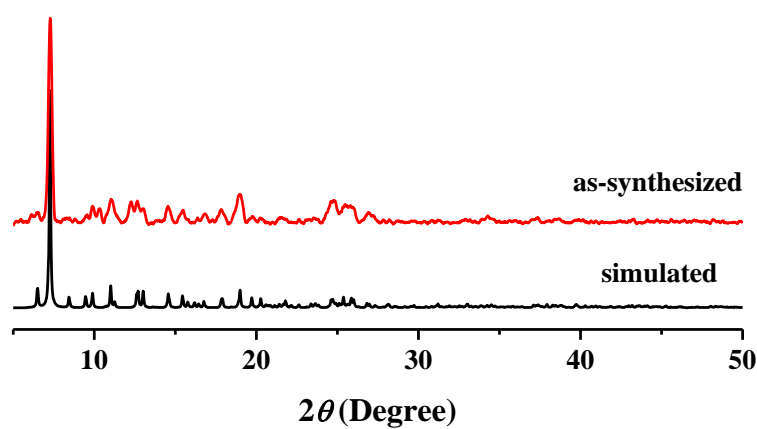


Figure S3. Simulated and as-synthesized PXRD patterns of compound **2**.

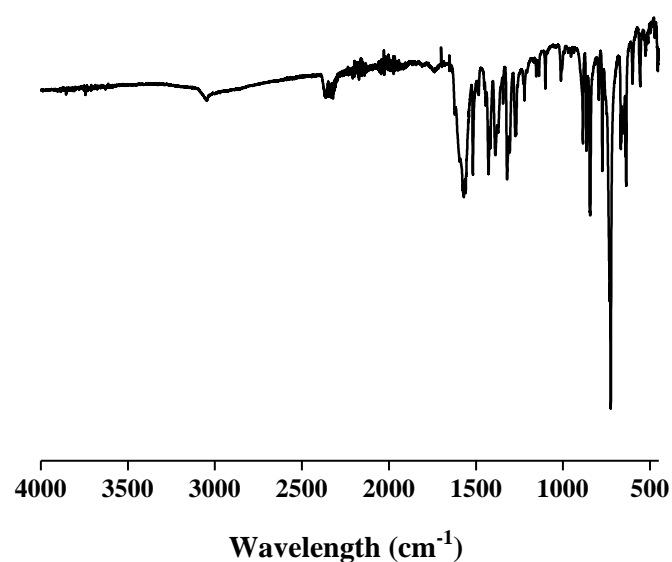


Figure S4. FT-IR spectrum of **2**.

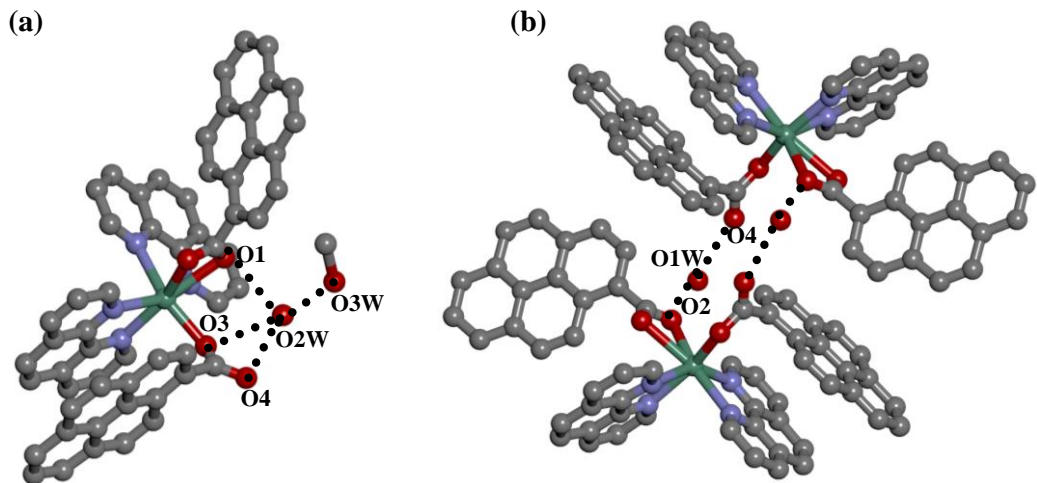


Figure S5. Hydrogen bonds (dotted black lines) in **1**: (a) $O_3 \cdots O_{2W}$, $O_4 \cdots O_{2W}$, $O_1 \cdots O_{2W}$ and $O_{2W} \cdots O_{3W}$ hydrogen bonds keep the guest solvents attached; (b) $O_4 \cdots O_{1W}$ and $O_2 \cdots O_{1W}$ hydrogen bonds hold two monomer complexes.

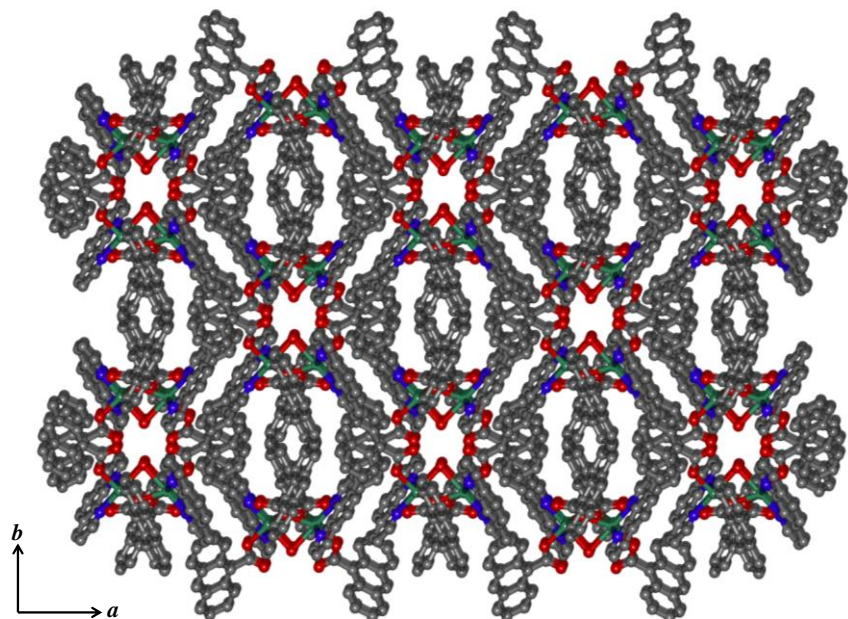


Figure S6. View of the 3D close packed structure of complex **2** along *c*-direction.

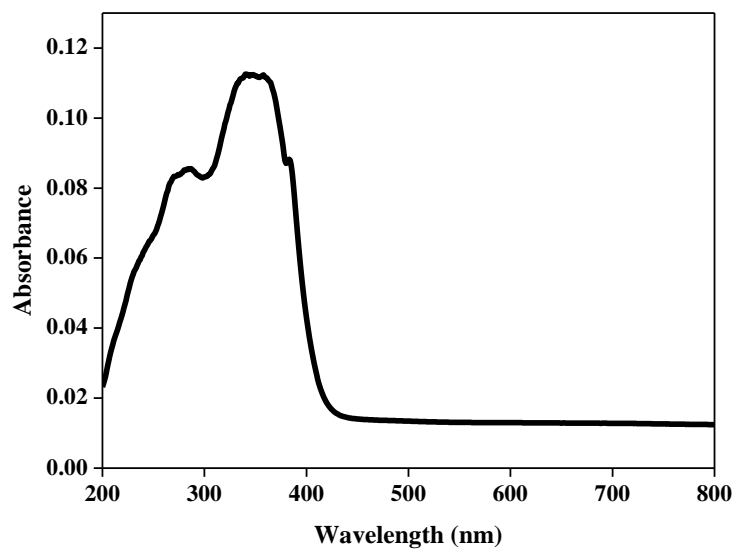


Figure S7. UV-vis spectrum of **1**.

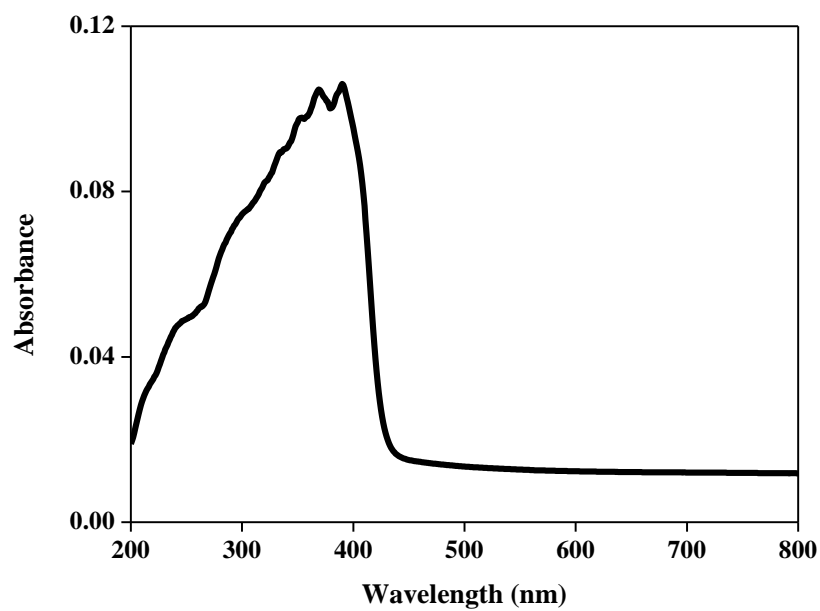


Figure S8. UV-visible spectrum of **2**.

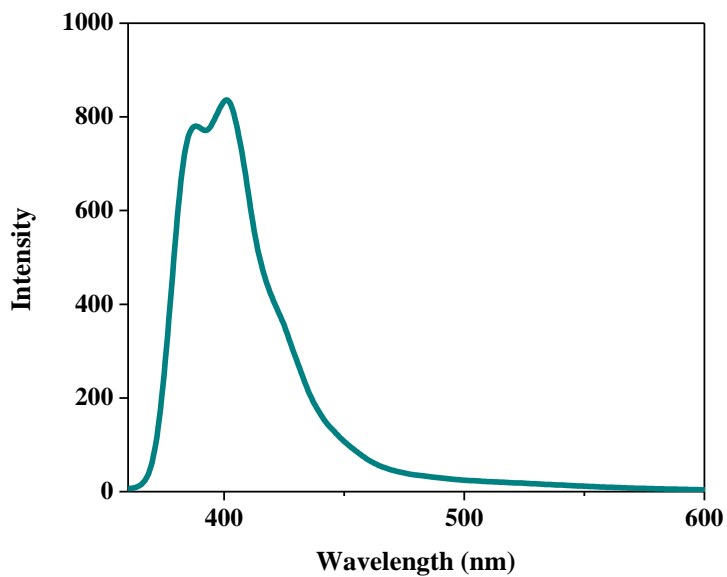


Figure S9. Emission spectrum of compound **1** in methanol upon excitation at 350 nm.

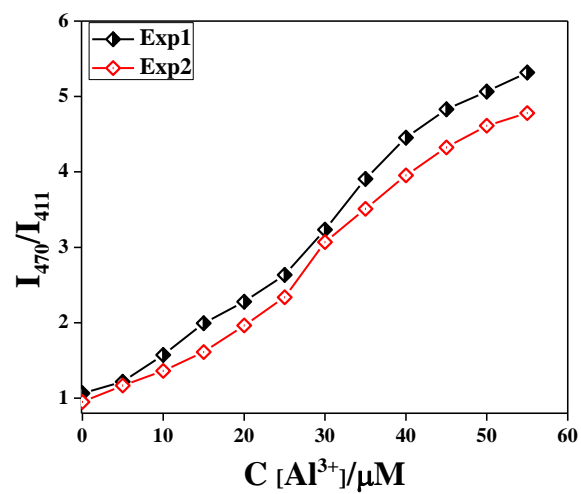


Figure S10. Ratiometric fluorescence intensity $[I_{470}/I_{411}]$ as a function of Al^{3+} concentration in methanol solution of compound **2**.

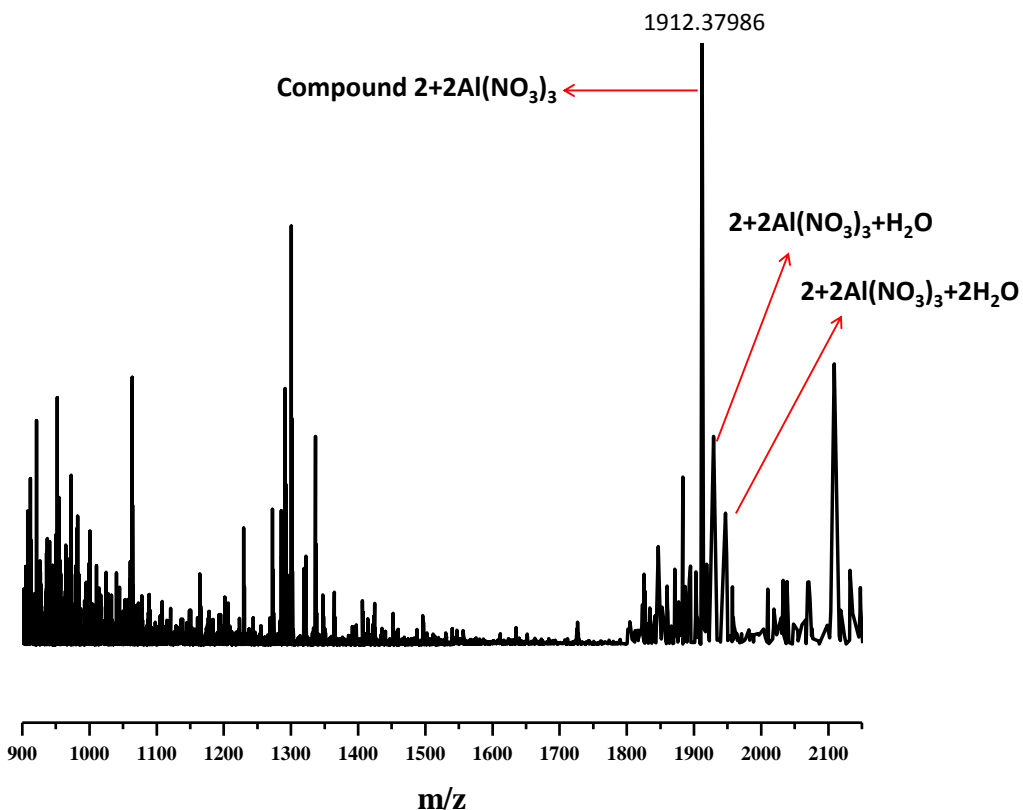


Figure S11. High Resolution Mass spectrum of Al^{3+} added compound **2** in methanol.

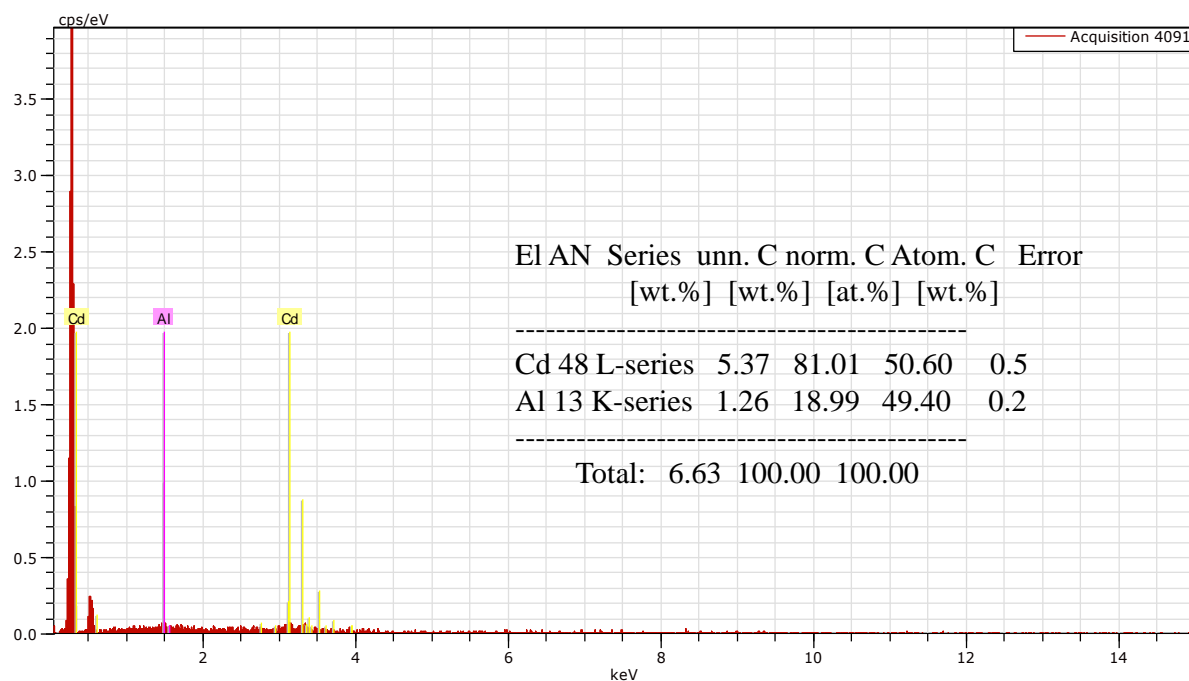


Figure S12. EDAX spectrum showing the Al^{3+} and Cd^{2+} abundance in **2** after Al^{3+} addition.

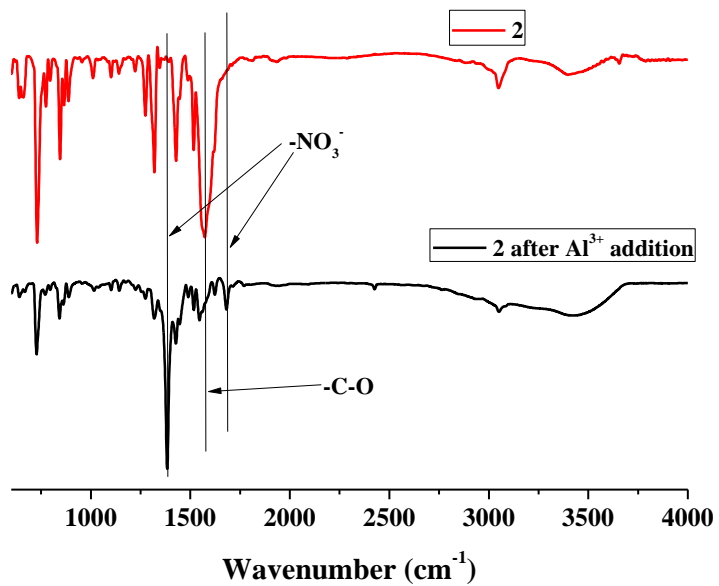


Figure S13. FT-IR spectrum of **2** and **2** after Al^{3+} addition.

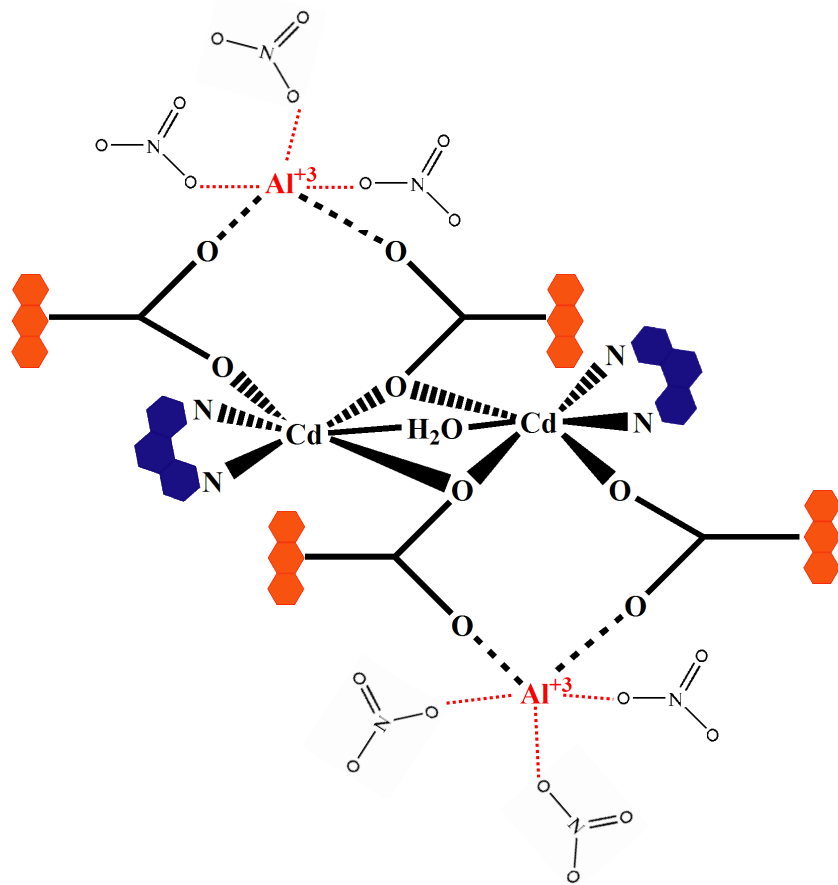


Figure S14. Possible interactions of Al^{3+} with the pendant oxygens in complex **2**.

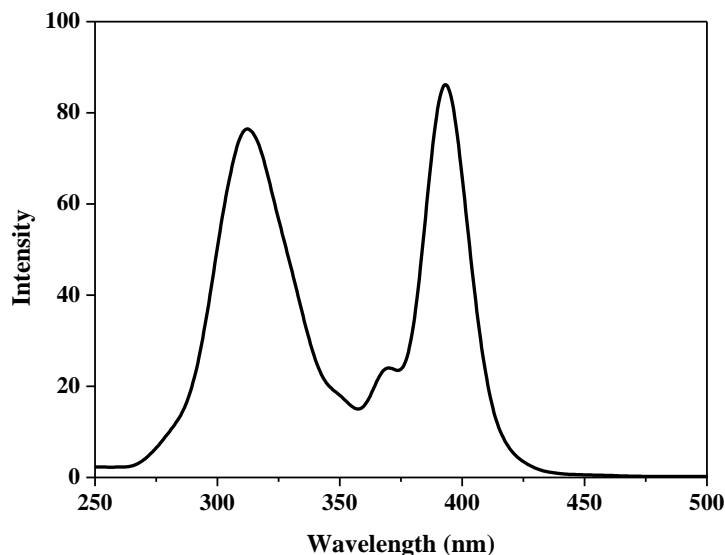


Figure S15. Excitation spectrum of methanol solution of compound **2** after addition of Al^{3+} , monitored at 510 nm.

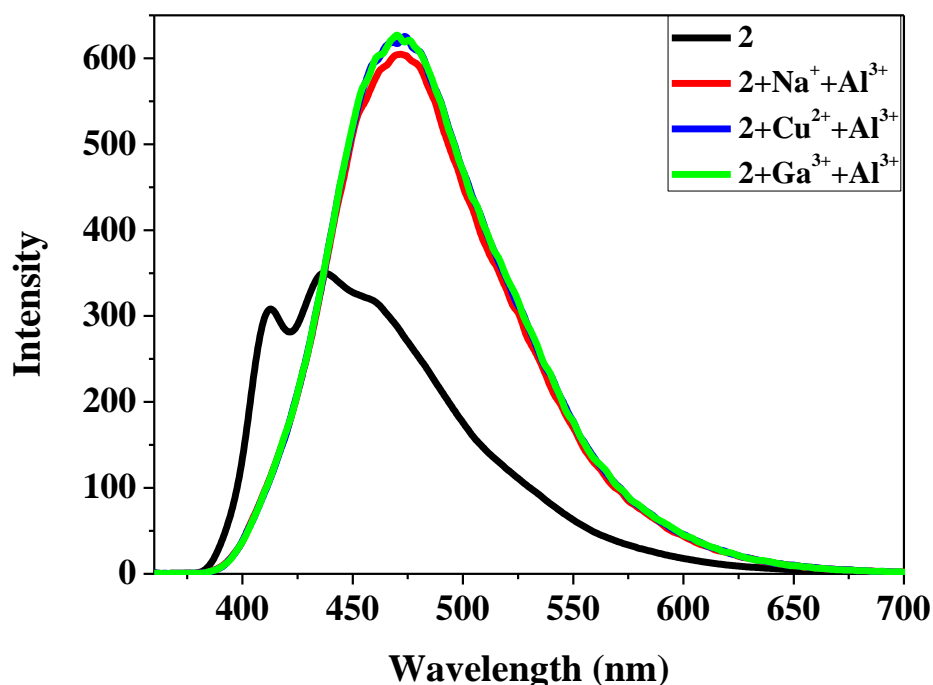


Figure S16. Emission spectra of methanol solution of compound **2** after addition of $\text{Na}^{+}+\text{Al}^{3+}$, $\text{Cu}^{2+}+\text{Al}^{3+}$ and $\text{Ga}^{3+}+\text{Al}^{3+}$ in 1:1 ratio upon excitation at 350 nm.

Table S1: Calculated CT transfer spectra (in nm) of compound **1** and compound **2** using different exchange correlation energy functional. Oscillator strengths are written in bracket.

System	CAM-B3LYP			B97XD			B3LYP		
	CT	$\pi - \pi^*$	$\pi - \pi^*$	CT	$\pi - \pi^*$	$\pi - \pi^*$	CT	$\pi - \pi^*$	$\pi - \pi^*$
pyrene	381.50 (0.03)	343.64 (0.28)	314.39 (0.24)	365.08 (0.04)	339.97 (0.29)	312.84 (0.29)	-	354.89 (0.18)	342.60 (0.09)
anthracene	356.70 (0.09)	333.21 (0.23)	323.61 (0.14)	349.91 (0.12)	331.78 (0.29)	316.31 (0.09)	-	378.46 (0.14)	370.49 (0.18)

The charge transfer (CT) spectrum was not observed using B3LYP exchange correlation energy functional. These results indicate the important of consideration of long-range corrected exchange correlations energy functional, CAM-B3LYP and B97XD in our study.

Table S2: Metal ion concentrations obtained by ICP analysis in metal bound compound **2** via dissolution of the compounds in water.

Metal ions	Concentrations mg/L
Na ⁺	3.705
Fe ³⁺	1.598
Zn ²⁺	1.159
Ga ³⁺	2.569
Cu ²⁺	2.177
Mn ²⁺	1.218
Eu ³⁺	5.136

Table S3: Cd²⁺ and Al³⁺ concentrations obtained by ICP analysis in compound **2** and metal bound compound **2** via dissolution of equal amount of compound **2** in water. Concentrations were measured in two different batches of experiments.

Compounds	Batch	Al ³⁺ mg/L	Cd ²⁺ mg/L
Compound 2	i	-----	2.850
	ii	-----	2.902
Al ³⁺ bound compound 2	i	2.635	2.795
	ii	2.560	2.817